33RD CONGRESS
OF THE INTERNATIONAL COUNCIL
OF THE AERONAUTICAL SCIENCES
STOCKHOLM, SWEDEN, 4-9 SEPTEMBER, 2022

Set-based Design Coordination between Coupled Systems: A Wing Aero-structural Design Perspective

Xin Chen, Atif Riaz, Marin D. Guenov

Centre for Aeronautics, Cranfield University, Cranfield, MK43 0AL, United Kingdom

Abstract

Presented in this paper is a novel, set-based method for design coordination between coupled systems. The research is motivated by the limitations of current point-based and set-based coordination approaches used as enablers for collaborative and interactive design. The proposed method employs design space exploration and surrogate models to process each sub-system in parallel. A combinatorial design of experiment is then performed, using the surrogate models and fixed-point iterations to solve the coupled systems. The result is a set of consistent and feasible solutions. The proposed approach was evaluated with a realistic wing aero-structural design problem. The result (a feasible set) is identical to the one produced by the benchmark studies, using the traditional monolithic setup. Compared with the latter, the proposed method enables distributed and parallel computation of the involved disciplines. Compared with the point-based approach, the proposed method shows to be more interactive and flexible by providing multiple promising design solutions.

Keywords: Design Coordination, Set-based Design, Distributed Design Collaboration, Wing Aero-Structural Design, Surrogate Modelling

1. Introduction

Design of complex systems such as aircraft involves the integration of various disciplines such as aerodynamics, structures, propulsion, flight control, and so forth. Within each discipline, modelling and simulations (M&S) are widely used to perform analysis and support decision making. Ideally, if these models from different domains are connected as an automatic workflow, optimization could be applied to search for solutions, which are optimal in terms of performance while fulfilling all the design requirements. However, such an All-in-One (OIA) process is generally not applicable in practice, due to the following reasons:

- The computational models of the different disciplines are normally hosted on distributed repositories, as these models may be created by designers/teams from separate departments or even distinct companies. Because of certain technical issues (e.g., automatic data exchange) or concerns about Intellectual Property (IP) protection, it can be very difficult to integrate all the models in one optimization problem.
- The All-in-One optimization process leads to a high dimensional combinatorial design space, which makes it very difficult for the optimizer to effectively search for the optimal values of design variables.

To overcome these challenges, various distributed architectures [1] have been developed within the context of Multi-disciplinary Design Optimization (MDO). These include Concurrent Subspace Optimization (CSSO) [2], Bi-level Integrated System Synthesis (BLISS) [3], Collaborative Optimization (CO) [4], Analytical Target Cascading (ATC) [5], etc. While the effectiveness of these design coordination methods has been proved in various applications [6–8], there are still limitations due to the Point-based Design (PDB) paradigm adopted in these optimization approaches:

- Inherent uncertainty associated with models, assumptions, and even requirements, especially at the early stage of design [9–11]. Therefore, the "optimal" solution may become less competitive or even infeasible at a later phase of the design process. This could result in compromised overall performance and/or costly re-design iterations.
- Once the optimization problem is formulated, the searching process is relatively less interactive and provides only limited knowledge of the design space. For example, it is difficult to identify trends between variables or extract design rules, given only the "optimal" solution.

For these reasons, the Set-based Design (SDB) paradigm has emerged as a result of research conducted in the last few decades [12–21]. Instead of searching for an "optimal" solution (which may become invalid later), the philosophy of SDB is to delay critical decisions by maintaining a set of feasible (and promising) solutions. In case of changing/adding requirements or revision of any analysis results, the designer only needs to narrow down the selections by gradually discarding infeasible (and uncompetitive) solutions. It is claimed that this approach avoids expensive re-design iterations.

In the multi-discipline context, design coordination is enabled by finding an intersection of feasible design spaces of different disciplines (sub-systems), as illustrated by Figure 1 (a). A more specific aircraft design example is shown in Figure 1 (b), where three constraints are specified on flyover noise, sideline noise, and NOx emission, respectively. Each constraint defines a feasible region in the design space of wing area and span. The intersection of these feasible regions is a common area of design points which satisfy constraints from all the disciplines (indicated by the white region).

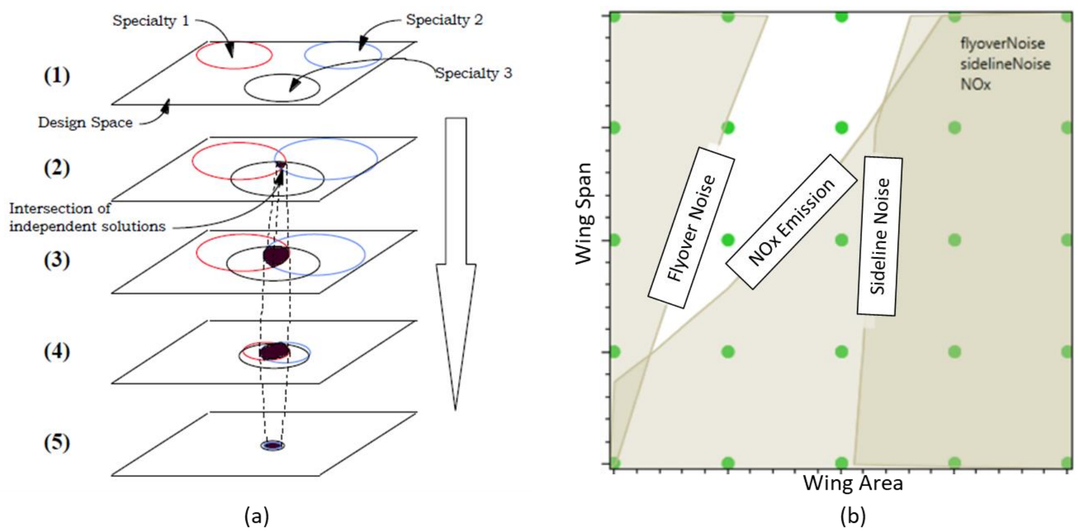

Figure 1 – (a) Intersection of feasible design spaces from different disciplines [20]. (b) An aircraft set-based design examples (adapted from [21])

However, the intersection can only be applied if there are shared design variables between the involved disciplines. That is, the design space must be defined with a common set of design variables. In this context, there is a research gap regarding the application of set-based methods for coordination of implicitly related and directly coupled disciplines, respectively. The former case refers to collaborative design where there are no direct input/output relationship between the disciplines, but some of the variables are correlated through a third discipline. For instance, the design of a wing's inner structure and high-lift movables can be implicitly linked by the actuation system located inside the wing structure. The latter case (coupled disciplines) refers to the design computation where feedback loops are formed between the inputs and outputs of different disciplines. A typical example is the wing aero-structural design problem where aerodynamic loads and structural deformation are dependent on each other in an iterative pattern.

In both cases, the intersection strategy is not applicable. This is because the implicitly coupled disciplines may not have any shared variables, while the coupled disciplines have an extra requirement on system consistency. That is, the values of each coupling variable should be identical in all the disciplines, or close enough (within a tolerance) for practical engineering implementation. Thus, a broader aim of the research presented here was to establish a general set-based framework to handle all these scenarios regarding design coordination. In this paper, the focus is particularly on coupled disciplines, while some initial research work for the general framework and implicitly related disciplines can be found in [19].

The rest of the paper is structured as follows: Section 2 defines the general design coordination problem of coupled disciplines with the help of a specific wing aero-structural design problem as an example. It also further explains why the intersection strategy is not applicable in this scenario. Section 3 presents the proposed set-based approach for coordination of coupled disciplines. In Section 4, the methodology is evaluated by using the aero-structural design problem as a test-case. Finally, conclusions are drawn, and future work is outlined in Section 5.

2. Problem Definition

2.1 General Problem

The general problem definition of horizontal design coordination is illustrated in Figure 2, where two disciplines (noted by subscript 1 and 2, respectively) are located at the same level in the product (discipline) decomposition hierarchy. Each discipline has some associated analysis models and local constraints, noted as functions f and g, respectively. To avoid cluttering, only inequality constraints are shown (the equality constraints have the same format). It can also be noted that no objective functions are defined, since the set-based approach is adopted. However, if the designer wants to identify a set of "promising" solutions regarding certain performance variables, the objectives can be formulated as constraints, where a lower or upper bound of the corresponding performance is specified.

The vectors of design variables are noted as $\boldsymbol{x}$, while the vectors of performance outputs are noted as $\boldsymbol{y}$. The variables can be divided into four categories: local design variables, shared design variables, implicitly related variables, and coupling variables. These categories are indicated by the superscript: l, s, i, and c, respectively. The local design variables are the inputs of only one discipline (indicated by the solid arrow in Figure 2) while the shared design variables are inputs of both disciplines (indicated by the dot-dashed arrow). The implicitly related variables may form some additional constraints beyond the scope of disciplines 1 & 2, as indicated by the dashed arrows. The focus of this research is the coupling variables. As indicated by the red double-dot-dashed arrows, $\boldsymbol{y}_1^{(c)}$ and $\boldsymbol{y}_2^{(c)}$ are produced as outputs of discipline 1 and 2, and are fed into the other discipline as inputs, respectively.

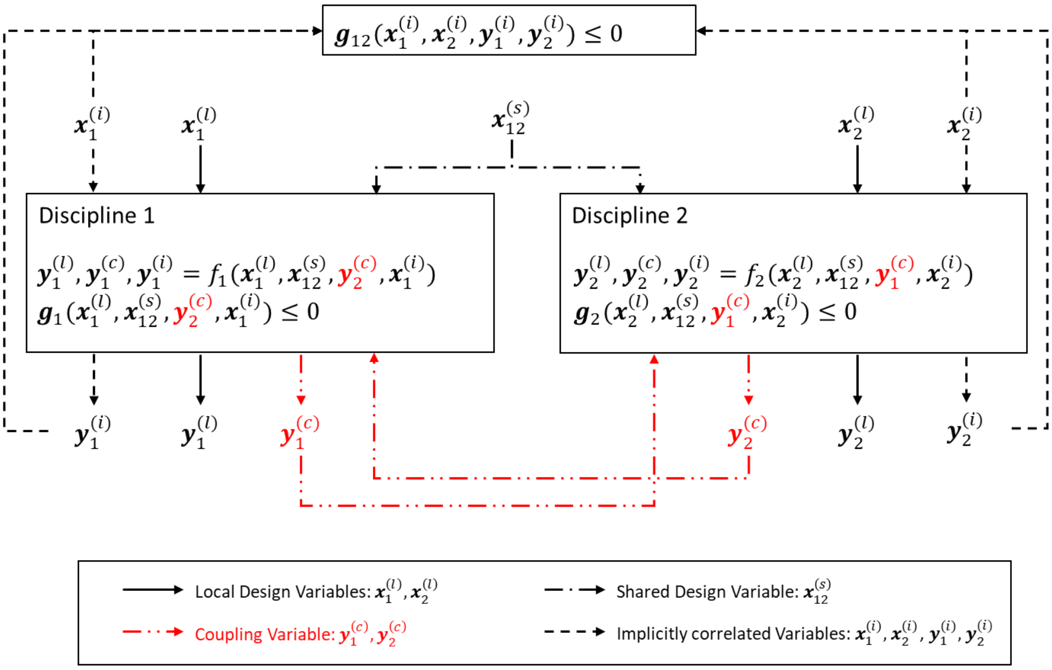

Figure 2 – General Problem Definition

Within this context, the aim of set-based horizontal design coordination is to identify a set of design solutions which fulfills the three requirements below:

- **Consistency**: The values of each coupling variable ($y_1^{(c)}$ and $y_2^{(c)}$) should be (ideally) identical in both disciplines, or close enough (within a tolerance) for engineering implementation.
- **Feasibility**: All the local and global constraints should be satisfied.
- **Optimality**: Ideally, the global optimal solution should be contained within the identified feasible region of design space.

2.2 Wing Aero-structural Design Problem

A typical example of coupled disciplines can be found in a wing aero-structural design problem, as illustrated in Figure 3 (a). Given a wing geometry, the aerodynamic model produces a vector of loads which are passed to the structural model. The latter computes the deformation of the wing structure which are then passed back to the aerodynamic model. As the deformation will change the wing geometry, the aerodynamic model has to be executed again, which provides a revised loads on the structure. Therefore, an iterative process is normally adopted to find a convergence point as illustrated in Figure 3 (b).

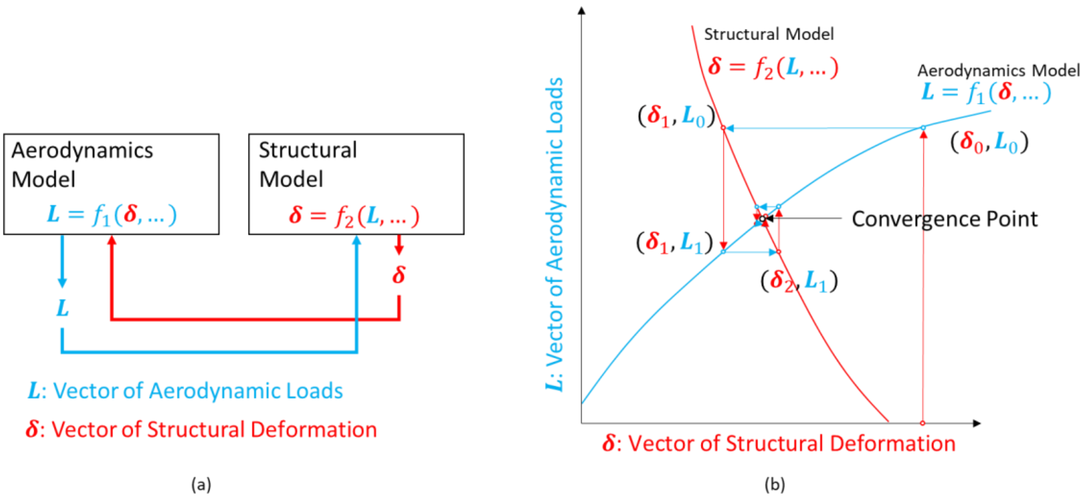

Figure 3 – (a) Coupling between aerodynamic and structural models. (b) Iterative process to solve the coupled systems

In this case, simply finding an intersected region in the space of aerodynamic loads and structural deformation, is not sufficient to produce the set of feasible design solutions, because it does not guarantee the system consistency. Specifically, the structural deformation and aerodynamic loads should be identical in both (aero and structural) models, respectively. As illustrated in Figure 4, a series of structural deformations are used as inputs of the aerodynamic model, which will produce a range of resulted aerodynamic loads. These values are indicated by the blue intervals on both axes. Similarly, a series of aerodynamic loads can be used as inputs to the structural model, which leads to a range of resulted structural deformations. These values are indicated by the red intervals on both axes. Although intersected intervals (indicated by green) can be found for both aerodynamic loads and structural deformations, all the solutions inside these intervals are actually invalid, except the convergence point.

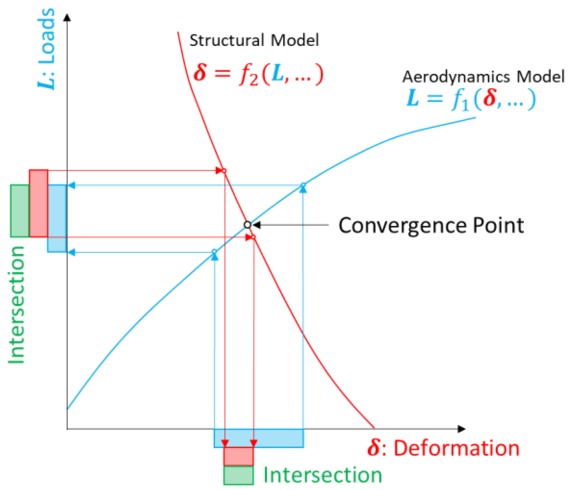

Figure 4 – Limitation of the intersection approach for coordination of coupled disciplines

3. Proposed Method

The proposed method is illustrated in Figure 5. The first step is to decouple the feedback loop by making a copy of the coupling variables in each discipline. As illustrated in Figure 6 (a), the copies of $\boldsymbol{y_1}$ and $\boldsymbol{y_2}$ in discipline 1 & 2 are noted as $\boldsymbol{y}_1^{(1)}, \boldsymbol{y}_2^{(1)}$ and $\boldsymbol{y}_1^{(2)}, \boldsymbol{y}_2^{(2)}$, respectively. Similar operation is also applied to produce the copies of the share design variables: $\boldsymbol{x}_{12}^{(1)}$ and $\boldsymbol{x}_{12}^{(2)}$. The implicitly related variables are not considered in this case, because they are out of the scope of this paper.

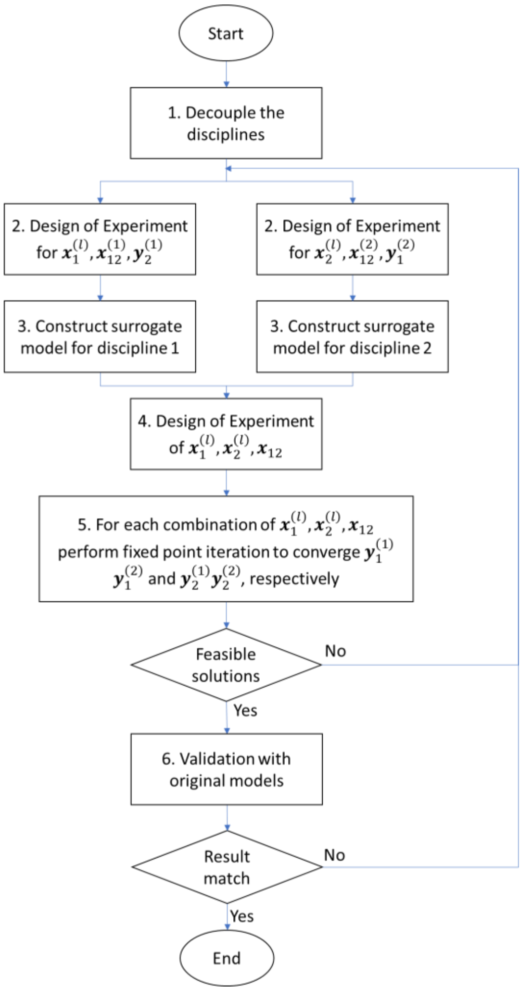

Figure 5 – Flowchart of the proposed method.

After being decoupled, the two disciplines can be considered as separated design problems, with $\boldsymbol{x}_1^{(l)}, \boldsymbol{x}_{12}^{(1)}, \boldsymbol{y}_2^{(1)}$ and $\boldsymbol{x}_2^{(l)}, \boldsymbol{x}_{12}^{(2)}, \boldsymbol{y}_2^{(2)}$ as their independent input variables, respectively. Step 2 is to perform a Design of Experiment (DoE) study for each discipline. For instance, in discipline 1, samples of $\boldsymbol{x}_1^{(l)}, \boldsymbol{x}_{12}^{(1)}, \boldsymbol{y}_2^{(1)}$ are produced and the models f_1, g_1 are executed for each sample. The results are then used to construct a surrogate model for discipline 1 in step 3. Similar operations are performed for discipline 2 in parallel.

In step 4, a combined DoE study is performed to produce samples of $\boldsymbol{x}_1^{(l)}, \boldsymbol{x}_2^{(l)}, \boldsymbol{x}_{12}$. In this step, there is no need to distinguish between $\boldsymbol{x}_{12}^{(1)}$ and $\boldsymbol{x}_{12}^{(2)}$, as they are shared in both disciplines. For each combination of $\boldsymbol{x}_1^{(l)}$, $\boldsymbol{x}_2^{(l)}$, and $\boldsymbol{x}_{12}$, fixed point iteration is then used to minimize the gap between copies of coupling variables in each discipline, as illustrated in Figure 6 (b). The local constraints also need to be evaluated with the surrogate models to ensure local feasibility.

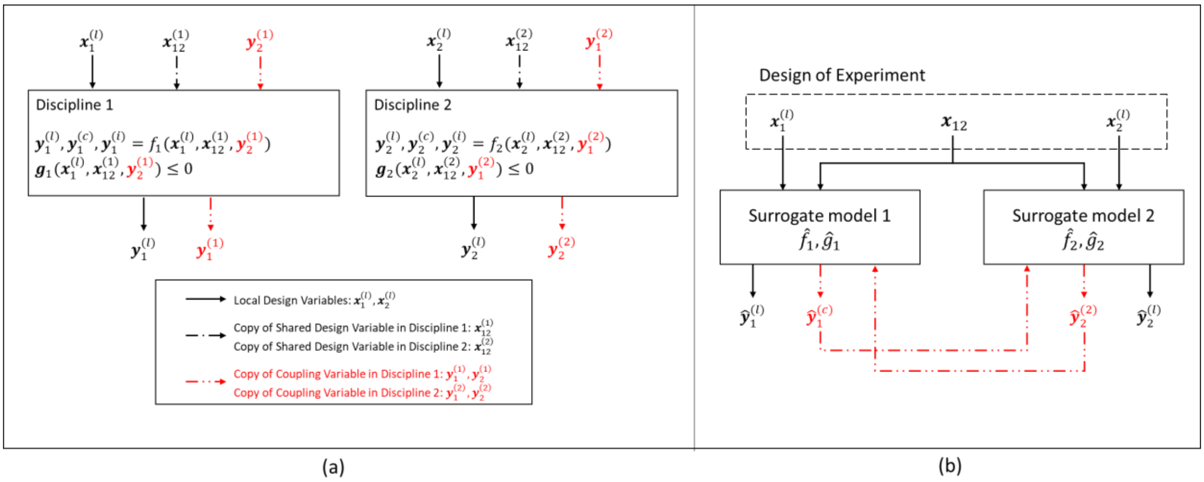

Figure 6 – (a) Decoupling of the disciplines. (b) Fixed point iteration to converge the coupling variables

After the DoE studies, a set of points should be produced in the design space of $\boldsymbol{x}_1^{(l)}, \boldsymbol{x}_2^{(l)}, \boldsymbol{x}_{12}$, $\boldsymbol{y}_2^{(1)}$ and $\boldsymbol{y}_1^{(2)}$, which satisfied the consistency requirement ($\boldsymbol{y}_1^{(1)} \approx \boldsymbol{y}_1^{(2)}$, $\boldsymbol{y}_2^{(1)} \approx \boldsymbol{y}_2^{(2)}$) and feasibility requirement ($g_1, g_2 \leq 0$), as discussed in Section 2. If there are no (or not enough) consistent and feasible solutions, step 2 should be repeated to further explore the design space. As the results produced so far are based on surrogate models, the two requirements (consistency and feasibility) need to be validated by calling the original models in step 6.

4. Evaluation

The proposed method is evaluated using a wing aero-structural design problem adapted from [22], where the spanwise distributions of twist, thickness to chord ratio, spar thickness, and skin thickness were optimized for minimum fuel burn. Each distribution is defined by a spline line with six control points along the semi-span. In the original problem, the wing planform was fixed and based on the NASA Common Research Model [23]. This is slightly modified in the current case study where wing planform parameters and dihedral angles are also considered as design variables. Meanwhile, the spanwise thickness to chord ratio is fixed to maintain the problem scale.

4.1 Decoupled Formulation

The aerodynamics and structural analysis are performed with an open-source tool named OpenAeroStruct (OAS) [22,24]. It should be noted that OAS itself has a built-in solver to handle the coupling between the two disciplines. In this evaluation, this solver is deliberately by-passed and the aero and structural analysis are wrapped into two separated models to demonstrate the distributed context.

Because of this separation, the coupling variables are converted into additional inputs and outputs for each discipline, respectively. For the aerodynamics model, the additional input is a matrix ($\boldsymbol{D}$) of displacement at each mesh nodes. Due to the high dimension of this matrix (corresponding to the spanwise nodes, chordwise nodes, and x, y, z directions), it is reformulated using a baseline ($\boldsymbol{D_B}$) and a series of scale factors ($\boldsymbol{K_D}$). The former is defined with an existing design point, for which the displacement matrix is already known. The scale factors are defined for the x, y, and z directions at 6 spanwise locations on the leading and trailing edges of the wing, respectively. A matrix of scale factors is defined as:

$$\boldsymbol{K_D} = \begin{bmatrix} k_{x_{LE_1}}, k_{x_{LE_2}}, \dots, k_{x_{LE_6}} \\ k_{y_{LE_1}}, k_{y_{LE_2}}, \dots, k_{y_{LE_6}} \\ k_{z_{LE_1}}, k_{z_{LE_2}}, \dots, k_{z_{LE_6}} \\ k_{x_{TE_1}}, k_{x_{TE_2}}, \dots, k_{x_{TE_6}} \\ k_{y_{TE_1}}, k_{y_{TE_2}}, \dots, k_{y_{TE_6}} \\ k_{z_{TE_1}}, k_{z_{TE_2}}, \dots, k_{z_{TE_6}} \end{bmatrix} \tag{1}$$

Figure 7 (a) illustrates the spline lines of scale factors for deformation in the z (vertical) direction along the leading and trailing edges. The other scale factors are not plotted to avoid cluttering. The baseline and scaled deformations of the wing are shown in Figure 7 (b). It should be noted that the scale values in this figure are arbitrarily selected for illustration purposes only.

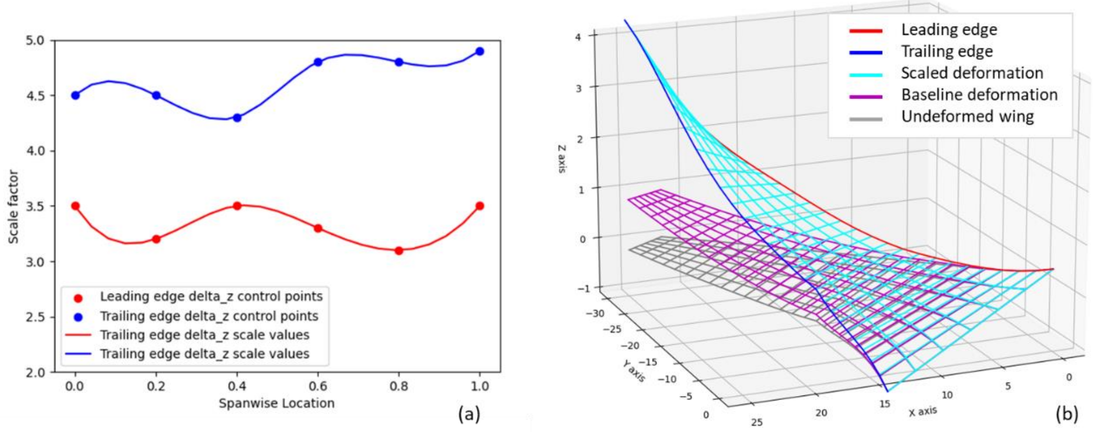

Figure 7 – Scaling of a baseline displacement matrix

The original coupling output from the aerodynamics model is a load matrix ($\boldsymbol{L}$), corresponding to the spanwise finite element nodes and 6 forces/moments along each axis ($\boldsymbol{F_x}, \boldsymbol{F_y}, \boldsymbol{F_z}, \boldsymbol{M_x}, \boldsymbol{M_y}, \boldsymbol{M_z}$). This matrix is also represented by a baseline and 6 scale factors for each of the 6 load dimensions.

$$\boldsymbol{K_L} = \begin{bmatrix} k_{x_{LE_1}}, k_{x_{LE_2}}, \dots, k_{x_{LE_6}} \\ k_{y_{LE_1}}, k_{y_{LE_2}}, \dots, k_{y_{LE_6}} \\ k_{z_{LE_1}}, k_{z_{LE_2}}, \dots, k_{z_{LE_6}} \\ k_{x_{TE_1}}, k_{x_{TE_2}}, \dots, k_{x_{TE_6}} \\ k_{y_{TE_1}}, k_{y_{TE_2}}, \dots, k_{y_{TE_6}} \\ k_{z_{TE_1}}, k_{z_{TE_2}}, \dots, k_{z_{TE_6}} \end{bmatrix} \tag{2}$$

Similar formulations are also applied for the decoupled structural model, but with a inversed setup for the loads and displacement matrices. The decoupled models are illustrated in Figure 8 and summarized in Table 1.

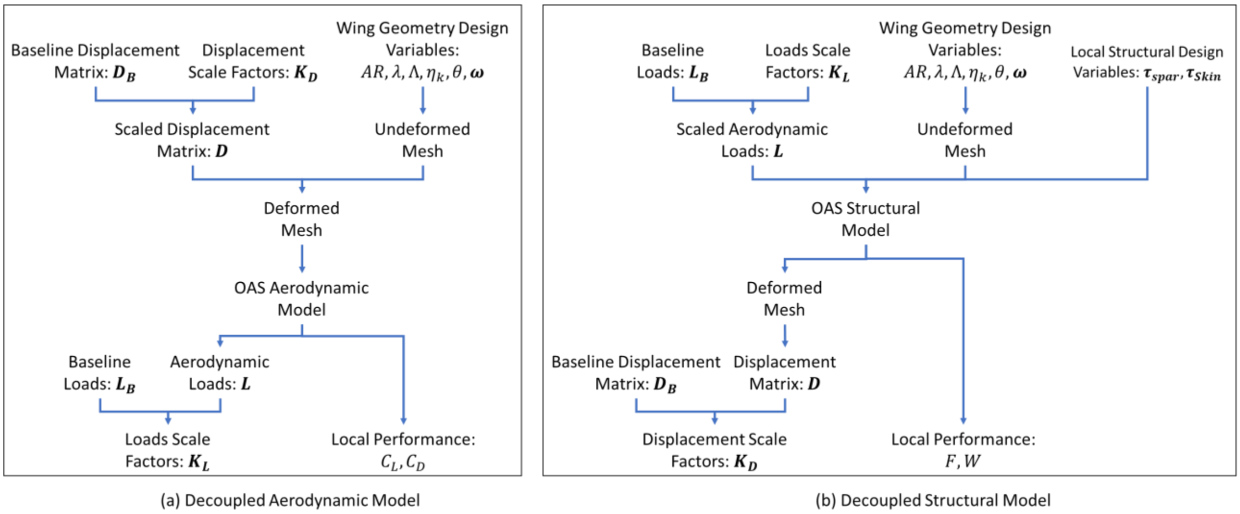

Figure 8 – Schematic view of the (decoupled) aero-structural design problem

Table 1 – Summary of the aerodynamic design problem

Category	Variable Name [Unit]	Symbol	DoE Range/Constraint
Shared Design Variables	Aspect Ratio	AR	$[8.50, 9.50]$
	Taper Ratio	λ	$[0.25, 0.30]$
	Quarter Line Sweep [degree]	Λ	$[33.00, 37.00]$
	Spanwise Location of the kink	η_k	$[0.36, 0.38]$
	Dihedral Angle	θ	$[0.00, 3.00]$
	Vector of Twist [degree]	$\boldsymbol{\omega}$	$[2.0, 9.0]$
Decoupled Input	Matrix of Displacement Scale Factors	$\boldsymbol{K_D}$	
Decoupled Output	Matrix of Load Scale Factors	$\boldsymbol{K_L}$	
Aerodynamic Local Performance	Lift Coefficient	C_L	$0.48 \leq C_L \leq 0.52$
	Drag Coefficient	C_D	

Table 2 – Summary of the structural design problem

Category	Variable Name [Unit]	Symbol	Range/Value
Shared Design Variables	Aspect Ratio	AR	$[8.50, 9.50]$
	Taper Ratio	λ	$[0.25, 0.30]$
	Quarter Line Sweep [degree]	Λ	$[33.00, 37.00]$
	Spanwise Location of the kink	η_k	$[0.36, 0.38]$
	Dihedral Angle	θ	$[0.00, 3.00]$
	Vector of Twist [degree]	$\boldsymbol{\omega}$	$[2.0, 9.0]$
Local Design Variables	Vector of Spar thickness [m]	$\boldsymbol{\tau_{spar}}$	$[0.003, 0.03]$
	Vector of Skin thickness [m]	$\boldsymbol{\tau_{Skin}}$	$[0.003, 0.03]$
Decoupled Input	Matrix of Load Scale Factors	$\boldsymbol{K_L}$	
Decoupled Output	Matrix of Displacement Scale Factors	$\boldsymbol{K_D}$	
Structural Local Performance	Failure Index	F	$F \leq 0$
	Wing Structural Mass [kg]	W	

4.2 Design of Experiment

With the two decoupled models, a Design of Experiment (DoE) study was performed for each discipline, respectively. The DoE results were then utilized to construct surrogate models as discussed in Section 3. In this case study, Artificial Neural Network (ANN) was selected due to its flexibility in handling high-dimensional nonlinear problems [25]. Specifically, Multi-layer Perceptron

(MLP) architecture with one hidden layer was adopted.

With the surrogate models, a DoE study was then performed within the combinatorial design space of shared and local design variables from both two disciplines. For each design points, the aerodynamic and structural surrogate models were employed to perform the fixed-point iteration.

4.2.1 Results Validation and Accuracy

Two benchmark studies were used to evaluate the proposed approach. The first benchmark DoE study was conducted by evaluating the same set of design points using the original models in a monolithic setup. The difference between the predicted values (y_{pred}) and reference values (y_{ref}) are measured by the Mean Relative Errors (MRE) and Weighted Mean Absolute Percentage Error (WMAPE) as defined in equations (3) and (4), respectively, where n is the number of design points and i is the index. The computed values of MRE and WMAPE for each output variables are shown in Figure 9 (a) and (b), respectively.

$$MRE = \frac{1}{n}\sum_{i=1}^{n}\frac{\left|y_{i_{pred}} - y_{i_{ref}}\right|}{\left|y_{i_{ref}}\right|} \tag{3}$$

$$WMAPE = \frac{\sum_{i=1}^{n}\left|y_{i_{pred}} - y_{i_{ref}}\right|}{\sum_{i=1}^{n}\left|y_{i_{ref}}\right|} \tag{4}$$

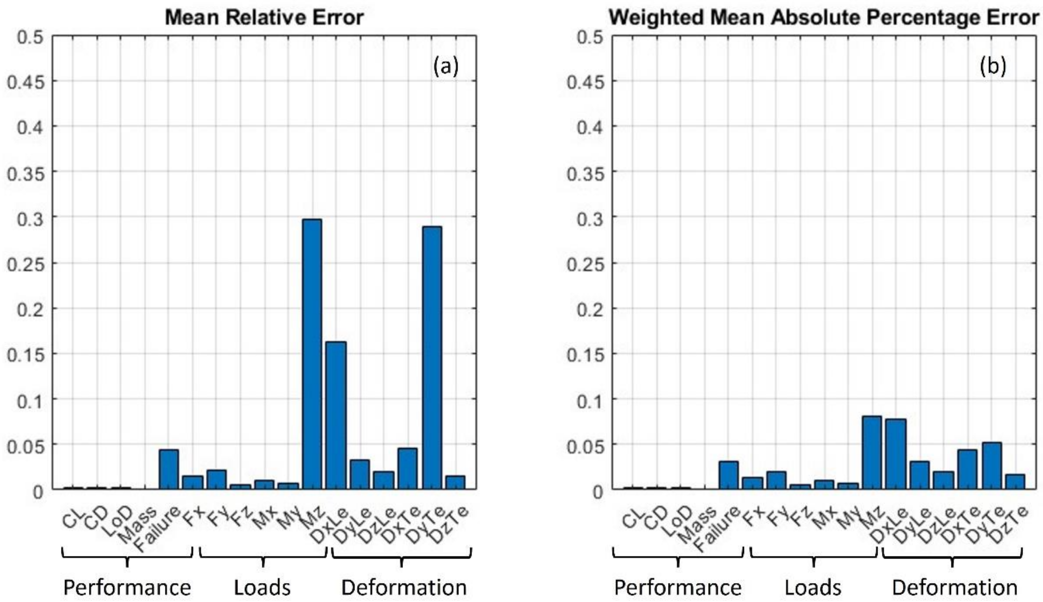

Figure 9 – Error for each output

In this case study, the error of each output is composed of three portions. The first portion is introduced by the surrogate models, and its magnitude is influenced by the number of training samples and specific setup of the surrogates. The second portion is caused by the scaling factors and spline lines for approximation of the load and displacement distributions, as discussed in Section 4.1. The last portion of error is due to the fixed-point iteration process, where the first two portions of error may be accumulated and amplified.

According to Figure 9, the error of bending moment along the z axis (M_z), leading-edge deformation along the x axis (Δx_{LE}), and trailing-edge deformation along the y axis (Δy_{TE}) are relatively higher than the other outputs. These errors are due to the nonlinearity of these output variables and error accumulation as discussed above.

It should be emphasized that the values of MRE can be misleading in this case study, because the denominator (y_{ref}) in equation (3) is very close to zero at some design points, which increases the MRE of the entire set of samples. This problem is mitigated by the formulation of WMAPE as defined in equation (4), and the latter is a more appropriate measurement of errors for such conditions. As illustrated in Figure 9 (b), the WMAPE of all the output variables are below 10%.

The DoE results from the proposed approach and benchmark study are visualised using the parallel coordinate plot [26] as shown in Figure 10, where each vertical coordinate is a dimension in the combinatorial design and performance space, while each polyline represents a design solution. In Figure 10, the feasible design solutions obtained from the benchmark study are marked in blue, while those obtained by the proposed approach are marked in green. The blue and green polylines are essentially overlapping in the design space, which indicates that the proposed approach has produced almost identical set of feasible solutions compared to the benchmark study. There are some slight differences in the performance space due to numerical errors as discussed above.

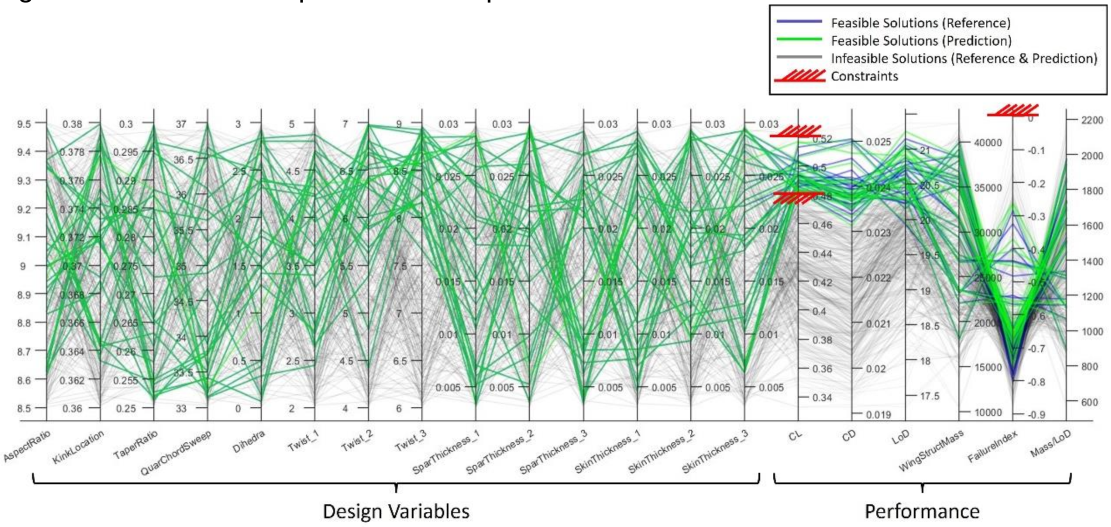

Figure 10 – DoE study using the original monolithic setup (blue) and distributed surrogate models (green).

4.2.2 Optimality and Flexibility

In the second benchmark study, a gradient-based optimization was performed to minimize the wing structure mass divided by the lift over drag. In Figure 11, the optimal solution is indicated by the magenta polyline and the feasible solutions produced by the proposed approach are marked in green.

In Figure 11 (a), the feasible solutions are based on a DoE study of 300 points and the optimum is outside the currently identified feasible region in the design space. An additional DoE study was then performed using 600 design points and the optimum is covered within the identified feasible region as shown in Figure 11 (b). In practice, as the optimal solution cannot be known *a priori*, it is not guaranteed to be included in the feasible design set. However, once the surrogate models have been constructed, the design space could be further explored without much additional computational cost. This would allow the feasible design set to expand gradually towards of the global optimum.

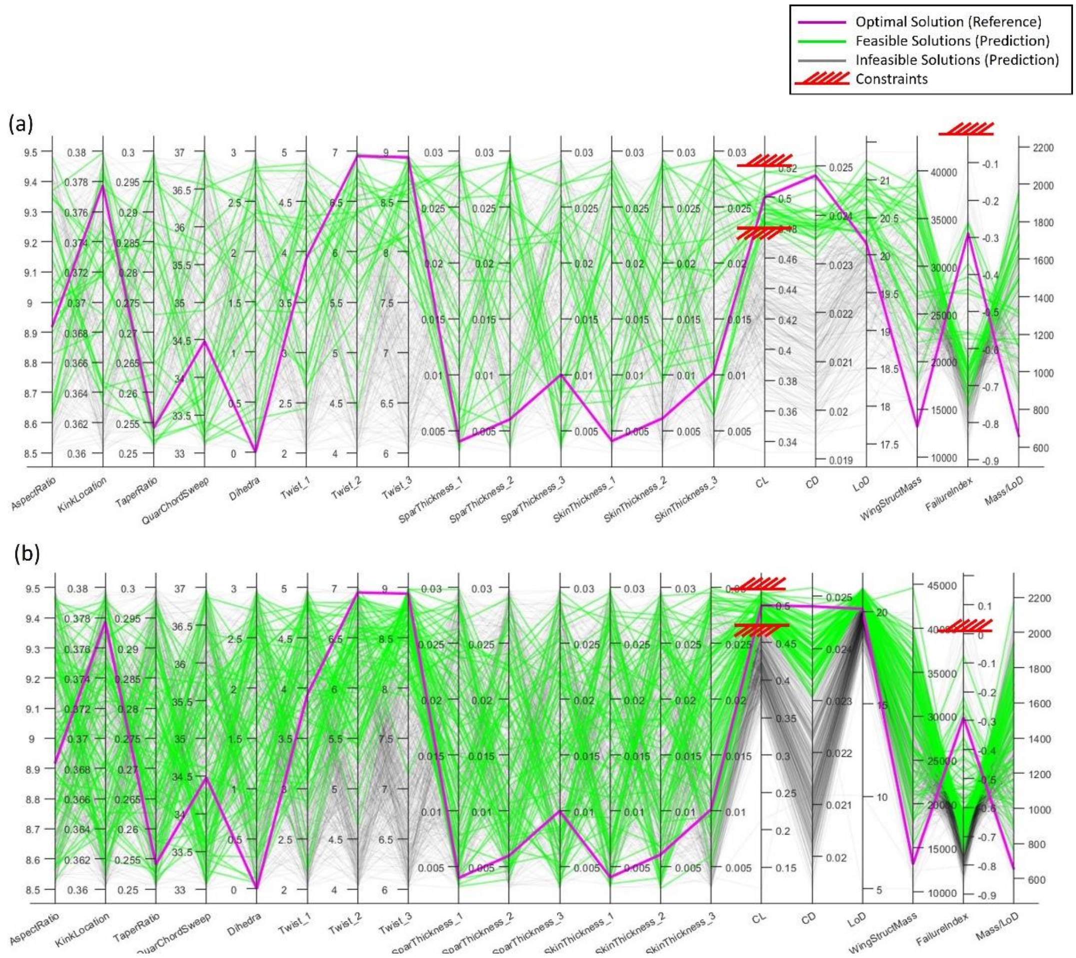

Figure 11 – Optimal solution from the second benchmark study in comparison with the feasible solutions from the proposed approach using (a) 300 design points, (b) 600 design points

The benefit of using set-based design approach is reflected on the flexibility for conducting trade-off studies. For instance, considering the uncertainty in the stress computation, a more stringent failure constraint could be defined as $F \leq -0.35$, instead of $F \leq 0$. In this scenario, the current optimum will become invalid, while the feasible design set could be reduced further according to the new constraint. Additional constraints can also be applied interactively on the drag coefficient and structural mass to filter out the non-promising solutions, as indicated in Figure 12.

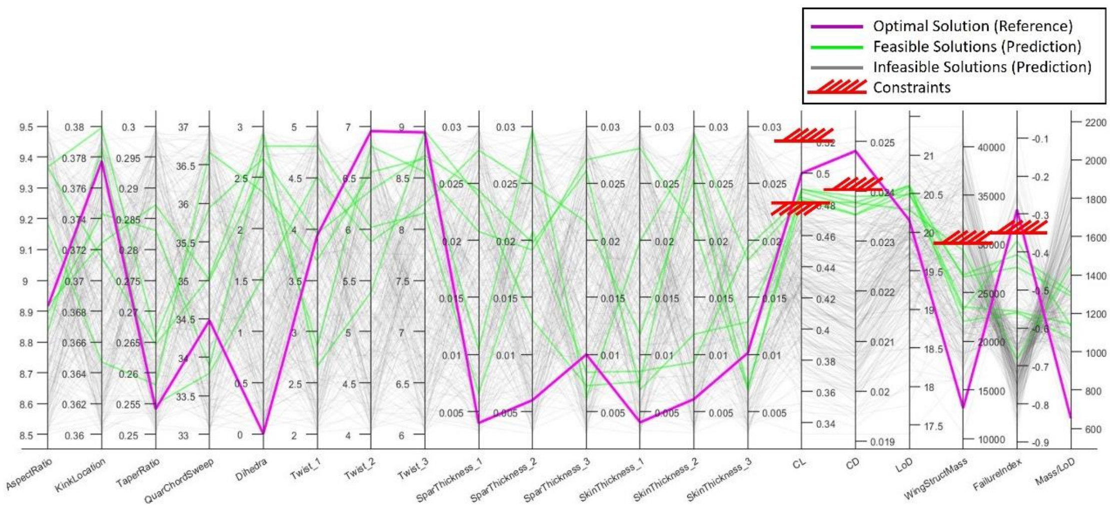

Figure 12 – Trade-off study with modified and additional constraints

4.2.3 Computational Cost

The computational cost is measured by the number of original model evaluations, and is largely dependent on the specific problem definition. The computation costs of the proposed approach and the two benchmark studies can be estimated using equations (5), (6), and (7), respectively. The specific numbers involved in this case study are summarized in Table 3.

$$N_P = N_{AeroTrain} + N_{StructTrain} + 2 \cdot N_{DoE} \quad (5)$$

$$N_1 \approx 2 \cdot N_{DoE} \cdot N_{FPI} \quad (6)$$

$$N_2 \approx 2 \cdot N_{OI} \cdot (1 + N_{FD}) \cdot N_{FPI} \quad (7)$$

Table 3 – Specific numbers of involved in this case study

Number of Points in	Symbols	Values	
Training aerodynamic surrogate	$N_{AeroTrain}$	1000	
Training structural surrogate	$N_{StructTrain}$	1000	
Combinatorial Design of Experiment	N_{DoE}	300	600
Fixed Point Iteration	N_{FPI}	10~30	
Optimization Iteration	N_{OI}	3	
Finite Differencing for Computing the Gradients	N_{FD}	14	
Total Number of Model Evaluations			
Proposed Approach	N_P	2600	3000
Benchmark 1: Monolithic Design of Experiment*	N_1	6564	13244
Benchmark 2: Monolithic Optimization	N_2	785	

* The numbers are corresponding to two DoE studies with 300 and 600 design points, respectively.

The computational cost of the proposed approach is mainly dependent on the number of samples used for training the surrogate models. In the combinatorial DoE study, fixed point iterations are performed with the surrogates. However, after convergence of each design point, the original models need to be invoked once again (without iterations) to validate the results, which leads to additional $2N_{DoE}$ model evaluations (for aero and structural analysis).

In the first benchmark study (monolithic design of experiment), the computational cost is equal to the number of design points in the outer DoE loop, multiplied by the number of fixed-point iterations in the inner loop. For most design points, the inner loop requires 10~30 iterations for convergences.

In the second benchmark study, the inner loop is still for fixed-point iterations, while the outer loop is used for searching the design space and computing the gradients (e.g. using finite differencing). In the current case study, the optimization stopped within only three 3 iterations, however, the gradient computation caused more model evaluations due to the high dimension of the design space. It should be mentioned that in the original setup of OpenAeroStruct, the gradients are computed in a more efficient way which can largely reduce the computational cost. This is currently beyond the scope of this paper, which considers a more general case, where the models are provided as black boxes.

5. Summary and Conclusions

Presented in this paper is a novel set-based method for (computational) design coordination of coupled systems. Although various monolithic and distributed architectures have been developed in the MDO context, the point-based optimization approaches are less flexible and non-interactive, thus not suited to handle early-stage design collaboration. On the other hand, the set-based coordination approaches rely heavily on design space intersection which is not applicable in the case of coupled disciplines. The proposed method aims to overcome of these limitations.

Specifically, the disciplines are first decoupled by making copies of the coupling and shared variables in each discipline (sub-problem). Then design space explorations are performed in parallel for each discipline. The results are used to construct surrogate models, which are later employed in a combinatorial design of experiment. The overall result is a set of consistent and feasible solutions.

The proposed approach was evaluated with a representative wing aero-structural design problem. The result (a feasible set) is virtually identical to the one produced by the benchmark study using the traditional monolithic setup. Compared with the monolithic set-based approach, the proposed approach enables distributed and parallel computation of the constituent disciplines. Compared with the point-based approach, the proposed approach enables flexible constraint allocation and iterative down selection of the design solutions. In this specific case study, the computational cost of the proposed approach is lower than the benchmark DoE study. This advantage will be more pronounced if extra design points are required for exploring the design space.

Some important (provisional) findings of this applied research are related to the use and reliance on the surrogate models in practice. Specifically:

- the numerical errors introduced by the surrogates accumulate in the iteration process.
- in this specific case study, the spline lines caused additional errors in the representation of the load and displacement distributions.
- in the monolithic setup, the values of the coupled variables are computed from iterations. However, after decoupling, the initial ranges of these coupled variables need to be assumed in each discipline. These assumed ranges will determine the training samples and could have a significant impact on the accuracy of surrogate models. Therefore, these assumptions need to be made with caution and require a substantial level of domain knowledge and experience.

Considering the above findings, future work includes three research directions. The first one is to explore other surrogate modeling techniques allowing to reduce the numerical errors. The second direction is to address the optimality requirement as specified in Section 2, which is currently not guaranteed in the proposed approach. The third direction is to develop a more adaptive method to identify the boundary between feasible and infeasible solutions.

Finally, a broader aim of our future work is to establish a general set-based design coordination framework to handle other generic scenarios, for instance, coordination of implicitly related disciplines and disciplines formed from different (product) decomposition levels.

Acknowledgment

The research leading to these results has received funding from Innovate UK, under the Collaboration Across Business Boundaries (COLIBRI) project (Ref no. 113296).

Copyright Statement

References

[1] Martins, J. R. R. A., and Lambe, A. B. Multidisciplinary Design Optimization: A Survey of Architectures. *AIAA Journal*, Vol. 59, No. 9, pp 2049-2075, 2013.

[2] Sobieszczanski-Sobieski, J. Optimization by Decomposition: A Step from Hierarchic to Non- Hierarchic Systems. *NASA/Air Force Symposium on Recent Advances in Multidisciplinary Analysis and Optimization*, No. NASA-TM-101494, 1988.

[3] Sobieszczanski-Sobieski, J., Altus, T. D., Phillips, M., and Sandusky, R. Bilevel Integrated System Synthesis. *AIAA Journal*, Vol. 38, No. 1, pp 164-172, 2000.

[4] Braun, R. D. *Collaborative Optimization: An Architecture for Large-Scale Distributed Design*. Doctoral dissertation, Stanford University, 1996.

[5] Kim, H. M., Michelena, N. F., Papalambros, P. Y., and Jiang, T. Target Cascading in Optimal System Design. *Journal of Mechanical Design*, Vol. 125, No. 3, pp 474-480, 2003.

[6] Ferez, R. E., Liu, H. H. T., and Behdinan, K. Evaluation of Multidisciplinary Optimization Approaches for Aircraft Conceptual Design. *10th AIAA/ISSMO multidisciplinary analysis and optimization conference*, Albany, New York, Vol 4, AIAA 2004-4537, pp 2574-2584, 2004.

[7] Ajmera, H. C., Mujumdar, P. M., and Sudhakar, K. MDO Architectures for Coupled Aerodynamic and Structural Optimization of a Flexible Wing. *45th AIAA/ASME/ASCE/AHS/ASC Structures, Structural Dynamics & Materials Conference*, Palm Springs, California, Vol. 1, AIAA 2004-1543, pp 365–375, 2004.

[8] Chell, B., Hoffenson, S., and Blackburn, M. R. A. Comparison of Multidisciplinary Design Optimization Architectures with an Aircraft Case Study. *AIAA Scitech Forum*, San Diego, California, AIAA 2019-0700, 2019.

[9] Yao, W., Chen, X., Luo, W., van Tooren, M., and Guo, J. Review of Uncertainty-Based Multidisciplinary Design Optimization Methods for Aerospace Vehicles. *Progress in Aerospace Sciences*, Vol. 47, No. 6, pp 450–479, 2011.

[10] Rocquigny, E. de., Devictor, Nicolas., and Tarantola, Stefano. *Uncertainty in Industrial Practice: A Guide to Quantitative Uncertainty Management*. John Wiley & Sons, Chichester, 2008.

[11] Zang, T. A., Hemsch, M. J., Hilburger, W., Kenny, S. P., Luckring, J. M., Maghami, P., Padula, L., and Jefferson, W. Needs and Opportunities Multidisciplinary Vehicles for Uncertainty- Design Methods for Aerospace. *NASA Technical Report*, No. NASA/TM-2002-211462, 2002.

[12] Sobek, D. K. D. K. I., Ward, A. C. A. C., and Liker, J. K. J. K. Toyota's Principles of Set-Based Concurrent Engineering. *MIT Sloan Management Review*, Vol. 40, No. 2, pp 67–84, 1999.

[13] Riaz, A., Guenov, M. D., and Molina-Cristóbal, A. Set-Based Approach to Passenger Aircraft Family Design. *Journal of Aircraft*, Vol. 54, No. 1, pp 310–326, 2017.

[14] Nunez, M., Datta, V. C., Molina-Cristobal, A., Guenov, M. D., and Riaz, A. Enabling Exploration in the Conceptual Design and Optimisation of Complex Systems. *Journal of Engineering Design*, Vol. 23, Nos. 10–11, pp 852–875, 2012

[15] Shallcross, N., Parnell, G. S., Pohl, E., and Specking, E. Set-Based Design: The State-of-Practice and Research Opportunities. *Systems Engineering*, Vol. 23, No. 5, pp 557–578, 2020

[16] Toche, B., Pellerin, R., and Fortin, C. Set-Based Design: A Review and New Directions. *Design Science*, Vol. 6, 2020.

[17] Kizer, J. R., and Mavris, D. N. Set-Based Design Space Exploration Enabled by Dynamic Constraint Analysis. *Proceedings of the 29th Congress of the International Council of the Aeronautical Sciences, ICAS*, St Petersburg, 2014.

[18] Shahan, D. W., and Seepersad, C. C. Bayesian Network Classifiers for Set-Based Collaborative Design. *Journal of Mechanical Design, Transactions of the ASME*, Vol. 134, No. 7, 2012.

[19] Chen, X., Riaz, A., Guenov, M. D., and Molina-Cristóbal, A. A Set-Based Approach for Coordination of Multi-Level Collaborative Design Studies. *AIAA Scitech Forum*, Orlando, FL, AIAA 2020-0320, 2020.

[20] Bernstein, J. I. *Design Methods in the Aerospace Industry: Looking for Evidence of Set-Based Practices*. Master dissertation, Massachusetts Institute of Technology, 1998.

[21] Guenov, M. D., Nunez, M., Molina-Cristóbal, A., Datta, V., and Riaz, A. Aircadia – an Interactive Tool for the Composition and Exploration of Aircraft Computational Studies At Early Design Stage. *29th Congress of the International Council of the Aeronautical Sciences*, St Petersburg, 2014.

[22] Chauhan, S. S., and Martins, J. R. R. A. Low-Fidelity Aerostructural Optimization of Aircraft Wings with a Simplified Wingbox Model Using OpenAeroStruct. *EngOpt 2018 Proceedings of the 6th International Conference on Engineering Optimization*, Lisbon, pp 418–431, 2018

[23] Vassberg, J. C., DeHaan, M. A., Rivers, S. M., and Wahls, R. A. Development of a Common Research Model for Applied CFD Validation Studies. *Collection of Technical Papers - AIAA Applied Aerodynamics Conference*, Honolulu, Hawaii, AIAA 2008-6919, 2008

[24] Jasa, J. P., Hwang, J. T., and Martins, J. R. R. A. Open-Source Coupled Aerostructural Optimization Using Python. *Structural and Multidisciplinary Optimization*, Vol. 57, No. 4, pp 1815–1827, 2018.

[25] Aggarwal, C. C. *Neural Networks and Deep Learning*. Springer, 2018.

[26] Inselberg, A. *Parallel Coordinates: Visual Multidimensional Geometry and Its Applications*. Springer, New York, 2009.